ACS OMEGA

http://pubs.acs.org/journal/acsodf

Article

Effective Adsorptive Removal of Methylene Blue from Water by Didodecyldimethylammonium Bromide-Modified Brown Clay

Muhammad Munir, Muhammad Faizan Nazar,* Muhammad Nadeem Zafar,* Muhammad Zubair, Muhammad Ashfaq, Ahmad Hosseini-Bandegharaei, Salah Ud-Din Khan, and Ashfaq Ahmad

Cite This: *ACS Omega* 2020, 5, 16711−16721

Read Online

ACCESS | Metrics & More | Article Recommendations | Supporting Information

ABSTRACT: In the present investigation, brown clay (BC) was modified with didodecyldimethylammonium bromide (DDAB) to produce a sorbent (DDAB-BC), which was characterized and applied for sorption of methylene blue (MB) from aqueous media. BC was functionalized using DDAB by cation exchange of the DDAB moiety with positive ions existing inside the interlayer spaces of the BC. X-ray diffraction (XRD) studies confirmed that the *d*-spacing of DDAB-BC became wider (3.39 Å) than that of BC (3.33 Å). Fourier transform infrared spectroscopy (FTIR) and scanning electron microscopy (SEM) were exploited to explore the functional groups and morphological structure of sorbents, respectively. The Brunauer−Emmett−Teller (BET) surface area, pore volume, and pore diameter of DDAB-BC were determined as 124.6841 m^2/g, 0.316780 cm^3/g, and 8.75102 nm, respectively. Batch sorption investigations were carried out to determine the optimum experimental conditions, using the one-factor one-time procedure. The sorption of MB on DDAB-BC strongly obeyed the Langmuir isotherm and agreed well with pseudo-second-order kinetics. Sorption of MB onto DDAB-BC showed maximum efficiency (~98%) and maximum sorption capacity (~164 mg/g) at optimal values of pertinent factors: dye concentration (100 mg/L), pH (7), and temperature (55 °C). Sorption isothermal studies predicted that removal of MB on DDAB-BC follows multilayer sorption at higher MB dye concentrations and monolayer sorption at lower MB dye concentrations.

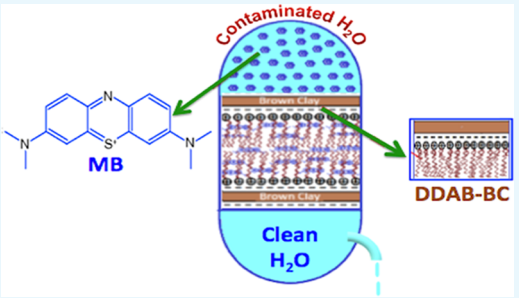

1. INTRODUCTION

Industrial revolution and expansion of occupational activities for the needs of bulk population have increased the environmental pollution. The contaminants and pollutants discharged from various industrial units are creating a threat to the life on the earth and atmosphere. Among all of the environmental pollutions, water pollution is of extraordinary concern. Leather and textile industries are the leading dyestuff consumers in Pakistan and therefore the main sources of dyeing waste.[1,2] The deterioration of aquatic environment by dye-containing effluents eventually affects aquatic fauna and flora. According to recent investigations, the researchers have reported that a total quantity of 7×10^5 tons of dyestuff is manufactured yearly and about 12−14% of which is discarded to the environment.[3]

Broadly, dyes are classified as anionic and cationic ones, on the basis of chemical functionality, and are toxic to a great extent and harmful to mankind and the environment. As they are having a toxic effect on the biotic component of the atmosphere, the investigators have tried their best to get rid of these pollutants. All available options have been employed to develop technologies for the abatement of water pollution caused by dyestuff. These technologies work via physicochemical,[4] biological,[5] ozonation,[6] membrane filtration,[7] advanced oxidation,[8] or integrated treatment processes,[4] but all of them have complete or partial limitations. Among these technologies, the process of adsorptive removal is groundbreaking, a cost-effective alternative, and easy to operate with a reliable performance.[9,10] Of countless sorbents used for the mentioned purpose, the most pertinent is the activated carbon, which unfortunately is accessible at high prices and is limited in amounts. Thus, many investigators are working to discover sustainable alternative sorbents such as agriculture waste, bagasse, and rice husk. However, these biosorbents need a number of physical and chemical modifications to improve their efficiency, in addition to their limited quantities.[11−13]

Simultaneously, clay sorbents are becoming popular for wastewater treatment.[14,15] Clay minerals possess distinct physical and chemical characteristics, which have transformed them into the ultimate choice for the sorption process due to being abundant in availability, low in cost, and classified as an environment friendly material. Therefore, clay can substitute low-performance biosorbents as well as costly activated

Received: April 8, 2020
Accepted: June 16, 2020
Published: June 29, 2020

carbon.[16] Clay sorbents may be used as such or in modified form depending upon the nature of the target pollutants.[17,18] Due to its geographical location, Pakistan possesses a great variety of clay minerals, and different types of clays abundantly exist in northern areas of this country, especially in the Azad Jammu and Kashmir (AJK) region.

A thorough literature survey reveals that no precise research study on the sorption potential of these clays, especially brown clay (BC), has been reported so far. Removal of organic pollutants from aqueous environments is primarily controlled by hydrophobic interactions at the interfaces of the sorbate and sorbent depending upon the carbon content of the sorbent rather than the mineral part of the clay sorbents.[19,20] The modification of clay can significantly improve its surface properties, thereby improving its water-decontaminating efficiency. Surface modification with quaternary ammonium salts (i.e., surfactants) causes the inversion of the surface charge of the clays, making them cation and anion exchangers, and facilitates the sorption of organic molecules that have less affinity toward the unmodified clay surface.[21]

Organoclays prepared by intercalating surfactants have a higher carbon content and enhanced hydrophobicity, especially when using a cationic surfactant like didodecyldimethylammonium bromide (DDAB) for intercalation.[22] In this way, cationic surfactants can exchange natural inorganic cations (sodium, calcium, potassium, and magnesium) on the clay surface, producing a carbon-enriched surface.[23] Intercalation of DDAB into the clay interlayers not only changes the hydrophilic environment to hydrophobicity but also greatly increases the interlayer spacing.[24,25] In addition, these organoclays are low-cost sorbents that can be used to treat most organic wastewater of the printing and dyeing unit.[26] Therefore, to achieve the above goal, BC was modified by DDAB, switching to an alternative organoclay, which has potential sorption characteristics including low cost, abundant availability, nontoxicity, and eco-friendly nature as well as enhancing the sorption capacity of BC for the sorption of methylene blue (MB) dye via intercalation of DDAB on the clay interspatial spaces.

MB is a basic dye (Figure S1) extensively used for cotton and silk painting. The most common harmful effect of MB is eye burn since it is thought to be the cause of permanent injury to eyes. It is also evident to cause mental confusion, profuse sweating, vomiting, nausea, breathing problem, and methemoglobinemia.[27] The present study was intended to investigate optimal values of various factors such as sorbent dose, particle size, pH, contact time, initial dye concentration, and temperature required for maximum removal of MB dye from aqueous environments. Furthermore, we have studied the sorption kinetic, equilibrium, and thermodynamics to understand equilibrium properties and the mechanism of the sorption process.

2. RESULTS AND DISCUSSION

2.1. Screening of Different Clays for Removal of MB.

The preliminary screening experiments have been performed to select the best clay with the highest sorption capacity for the removal of MB. For this purpose, eight different clays have been selected from various regions and tested for the sorption of MB. Eight flasks, labeled with clay names, with 100 mL of 50 mg/L MB solution each containing 0.04 g of clay samples are agitated in an incubator shaker for 60 min. The sorptive removal of MB is calculated, and results are illustrated in Figure 1. The results depict that the maximum sorption capacity for MB is shown by BC with respect to all other clay

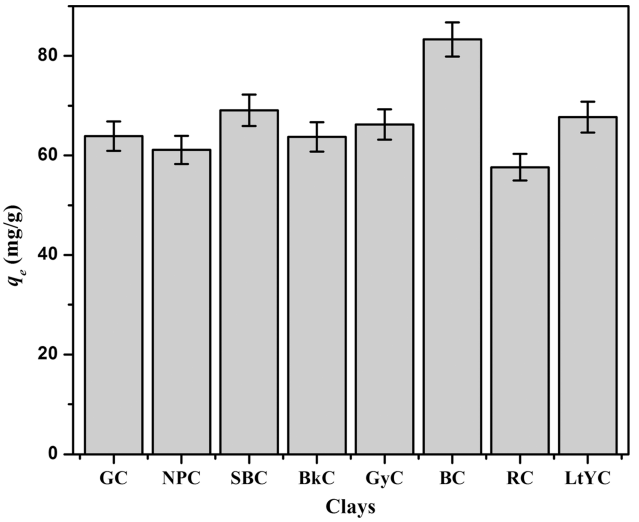

Figure 1. Comparison of sorption capacities of different clays: green clay (GC), natural pink clay (NPC), sky blue clay (SBC), black clay (BkC), gray clay (GyC), brown clay (BC), red clay (RC), and light yellow clay (LtYC).

samples; hence, BC is selected for modification in rest of the study. The BC is further modified with the DDAB surfactant to improve the sorption capacity of the clay, and a comparative study of raw BC and DDAB-modified BC is performed.

2.2. BC and DDAB-BC Characterization.

Visual assessment of scanning electron microscopy (SEM) images gives the morphology of the surface in BC and DDAB-BC sorbents and gives evidence about the textural properties of the sorbents. The SEM images of BC and DDAB-BC before MB sorption are displayed in Figure 2, and SEM images of MB-loaded BC and DDAB-BC are illustrated in Figure 3. The SEM image (Figure 2a) of the BC exhibits apparently the beads of nonmodified clay. In contrast, the DDAB-BC, synthesized by the interaction of cationic surfactant with clay mineral, is texturally more homogeneous, demonstrating that intraparticle areas have adequately been filled with the DDAB surfactant, as displayed in Figure 2b. Further, SEM micrographs of MB-loaded BC and DDAB-BC exhibit the complete filling of the sorption sites of the studied sorbents (Figure 3).

X-ray diffraction (XRD) is an excellent technique to compare the interlayer distance of BC and DDAB-BC sorbents. XRD spectra of BC and DDAB-BC sorbents are presented in Figure 4. The values of *d*-spacing for the most intense peak cantered at a 2θ value of about 26.50 are 3.33 and 3.39 Å for BC and DDAB-BC, respectively. The treatment of clay with DDAB results in an increase in the *d*-spacing, which could be due to the higher number of carbon atoms in DDAB. The higher *d*-spacing facilitates sorption of larger dye or phenol molecules, and it decreases diffusion resistance during the sorption process.[28,29]

The behavior and sorption capacity of BC and DDAB-BC can be forecasted from the information about porosity and surface area. The information of sorption isotherms of BC is presented in Figure S2 and Table S1, whereas the information of sorption isotherms of DDAB-BC is presented in Figure 5 and Table S1, which specify that all samples have exhibited a much longer straight-line portion of the curve. Surface area

https://dx.doi.org/10.1021/acsomega.0c01613
ACS Omega 2020, 5, 16711−16721

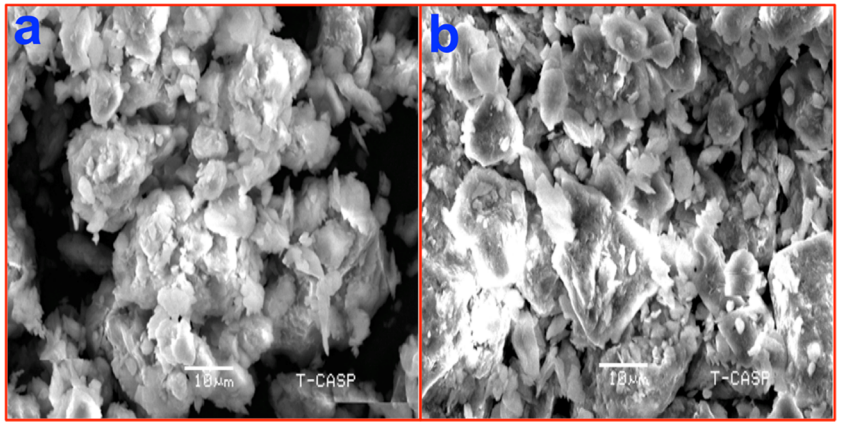

Figure 2. SEM images of (a) BC and (b) DDAB-BC before sorption of MB.

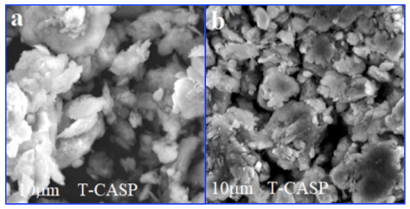

Figure 3. SEM images of (a) MB-loaded BC and (b) MB-loaded DDAB-BC after MB sorption.

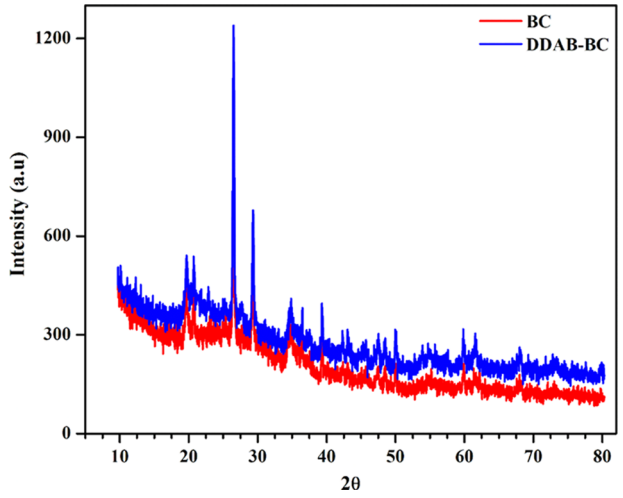

Figure 4. X-ray diffraction (XRD) patterns of BC and DDAB-BC.

analysis vouchsafes that the specific surface area of the DDAB-BC as determined by the Brunauer–Emmett–Teller (BET) procedure is much higher (124.6841 m^2/g) than that of BC (14.5884 m^2/g). The pore volume and the diameter of BC are determined to be 0.031916 cm^3/g and 10.16264 nm, respectively, whereas the pore volume and the diameter of DDAB-BC are determined to be 0.316780 cm^3/g and 8.75102 nm, respectively.

2.3. Effect of Solution pH. To investigate the influence of pH on MB sorption, the pH of the MB solution was varied from 2 to 11. The results of sorption behavior of MB at different pH values are illustrated in Figure 6a. The sorption studies demonstrate the enhanced sorption efficiency of MB from acidic to basic pH on both BC and DDAB-BC. An appreciable increase in dye uptake has been observed up to pH

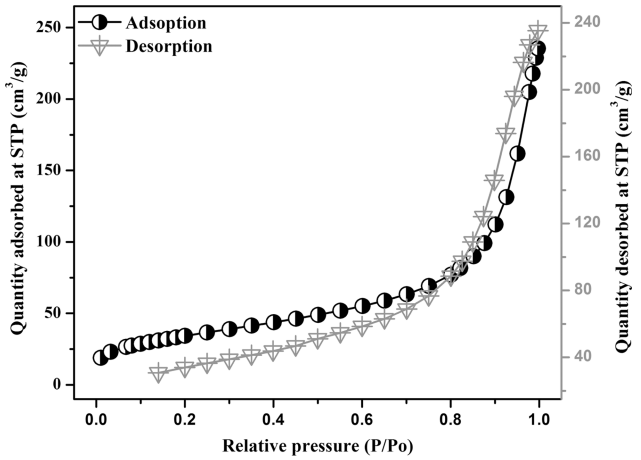

Figure 5. BET isotherm plot of the DDAB-BC sorbent.

7; thereafter, a slight decrease in the sorption of MB has been observed.

The variation in the sorption behavior of MB on BC and DDAB-BC with respect to initial pH alteration can be elucidated on the basis of point of zero charge (PZC) and molecular structure of MB. The PZC values for BC and DDAB-BC are determined to be 8.1 and 8.7, respectively (Figure S3). It is known that, as we move above pH_{pzc}, the adsorbent particles attain a negative surface charge. MB is basic in nature and remains in an ionized form up to pH 7.4 with positive surface charge. As the pH of the solution was increased from 2 to 7, the BC and DDAB-BC surface became more and more deprotonated, providing more and more sorption sites for MB with increased sorption efficiency. At above pH 7.4, MB exists in an unionized form with neutral surface. The BC and DDAB-BC surfaces acquire a negative charge above their PZC (pH_{pzc} 8.1 and 8.7). Therefore, it can easily be understood that electrostatic interactions along with the nonpolar interactions are responsible for the increase in dye uptake up to pH 7, and the decrease in electrostatic forces of attraction due to the neutral sorbate surface is credited for maintaining MB sorption at a steady rate above pH 7. The same trend has been supported by the literature for MB sorption.[30,31] Consequently, the pH 7.0 has been reflected to be the optimum level because at this pH the maximum sorption capacity (123 ± 2.5 mg/g for BC and 163 ± 4.2 mg/g for DDAB-BC) has been observed.

https://dx.doi.org/10.1021/acsomega.0c01613
ACS Omega 2020, 5, 16711−16721

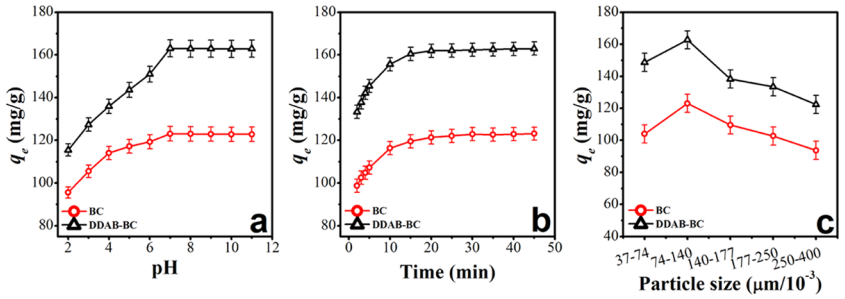

Figure 6. Effect of pH (a), time (b), and particle size (c) on sorption of MB onto BC and DDAB-BC.

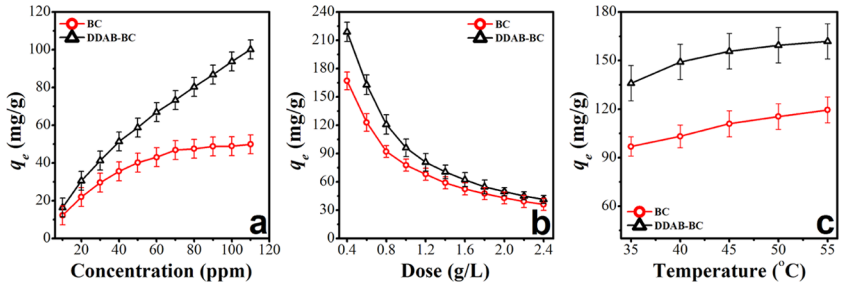

Figure 7. Effect of MB concentration (a), sorbent dose (b), and temperature (c) on sorption of MB onto BC and DDAB-BC.

2.4. Influence of Contact Time. The influence of contact time is a pertinent factor since it provides the relationship between fixed amounts of sorbent and contact time. It is utilized to estimate the sorption−desorption equilibrium contact time. The effect of time variation on the sorption capacity of BC and DDAB-BC for the removal of MB has been investigated in the range of 2−45 min as illustrated in Figure 6b. A rapid increase in the sorption capacity of both BC and DDAB-BC is noted during the first 10 min, and afterward, a very slow increase in the MB uptake is observed up to 45 min for both BC and DDAB-BC. The maximum sorption capacity (122.88 ± 2.7 mg/g for BC and 162.40 ± 3.2 mg/g for DDAB-BC) is determined at equilibrium time (30 min). The higher rates of sorption capacity of both BC and DDAB-BC at the beginning may be attributed to the presence of a large number of sorption sites at the surface of both BC and DDAB-BC, and low increase in sorption capacity is credited to the sorption sites existed in the internal regions of both BC and DDAB-BC. The enhanced sorption capacity of organoclay DDAB-BC could be due to surfactant modification, which has increased the carbon content of the sorbent.

2.5. Influence of Particle Size. A very important factor affecting the sorption behavior of MB is the size of particles of the sorbents (BC and DDAB-BC). The influence of particle size is studied by changing the particle size from 37 to 400 μm as illustrated in Figure 6c. An inverse relationship exists between the particle size of the BC and DDAB-BC and the sorption behavior of MB molecules because the surface area of sorbents increases with the decrease in particle size of the BC and DDAB-BC sorbents. A smaller particle size of the sorbent results in a higher sorption capacity of BC and DDAB-BC.[32] The sorbent size of about 74 μm is found to be optimum for BC and DDAB-BC. The maximum sorption capacities for BC and DDAB-BC are 123.05 ± 2.3 and 162.72 ± 4.1 mg/g, respectively. Afterward, the reduction in particle size shows no appreciable increase in the removal of MB. These studies have provided a firm basis to believe that sorption capacity is increased up to a definite particle size, below which it remains invariable. Thus, the smallest particle size of 74 μm was utilized for further studies.

2.6. Influence of Initial Dye Concentration. The initial dye concentration is another important factor, which controls the sorption behavior of the dye. The influence of initial dye concentration has a relationship with the available sorption sites on the surface of the sorbent. The effect of MB concentration (10−110 mg/L) on the sorption capacity of BC and DDAB-BC is shown in Figure 7a. Experimental investigations reveal that on varying the sorbate MB concentration from 10 to 110 mg/L, the sorption capacity is increased from 16.25 ± 0.8 to 120.14 ± 2.9 mg/g in the case of BC and from 16.57 ± 1.2 to 160.87 ± 4.4 mg/L in the case of DDAB-BC. Similar results have been reported in the literature.[33,34] The quantity of sorption sites at the surface of BC and DDAB-BC is greater, in the case of lower MB concentration, as compared to the MB molecules available; consequently, the majority of the MB molecules are adsorbed at the surface of the BC and DDAB-BC. Thus, a high percentage of MB molecules is adsorbed and high sorption efficiency is noted (results not shown) but low sorption capacity due to smaller amount of MB molecules available for both BC and DDAB-BC. Contrarily, in the case of higher concentrations of MB, the number of active sorption sites present on the surface of BC and DDAB-BC are smaller than the quantity of MB molecules available; thus, sorbate molecules have to compete among themselves for the fixed quantity of sorption sites on the surface of BC and DDAB-BC. Resultantly, the excess amounts of the sorbate molecules remain unsuccessful to be adsorbed on the surface of BC and DDAB-BC and stay free in the solution. Therefore, sorption capacity is increased while sorption efficiency (results not shown) is decreased with the increase of the concentration of MB. The study of the effect of MB concentration again shows clearly that sorption capacity is extremely higher for DDAB-BC compared to BC.

2.7. Influence of BC and DDAB-BC Dose. To study the effect of sorbent dose, the quantity of the sorbent is varied

https://dx.doi.org/10.1021/acsomega.0c01613
ACS Omega 2020, 5, 16711−16721

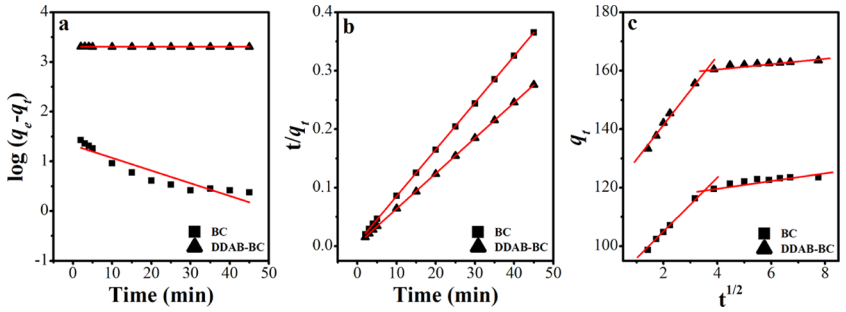

Figure 8. Pseudo-first-order model (a), pseudo-second-order model (b), and intraparticle diffusion model (c) for MB sorption onto BC and DDAB-BC.

from 0.4 to 2.4 g/L, and the results are shown in Figure 7b. The results illustrate that in the case of BC the sorption potential decreases from 167.02 ± 4.7 to 36.14 ± 1.3 mg/g and sorption efficiency increases from 66.81 to 88.72% (results not shown) when the quantity of BC is increased from 0.4 to 2.4 g/L. A similar trend is also observed for DDAB-BC, that is, the sorption capacity of DDAB-BC decreases from 218.88 ± 6.2 to 41.41 ± 1.2 mg/g and the sorption efficiency increases from 87.56 to 99.38% (results not shown) on increasing the amount of DDAB-BC from 0.4 to 2.4 g/L, but further increment of the sorbent dose does not show any change in the sorption efficiency of DDAB-BC because majority of fixed number of dye molecules are adsorbed on excess number of sorption sites and negligible number of dye molecules are left. A similar trend has also been reported elsewhere.[35−37] The maximum MB sorption was found at 0.6 g/L sorbent dose for both BC and DDAB-BC.

2.8. Influence of Temperature. The temperature change could derive the diffusion of MB molecules on the sorption sites present at the surface and inner porous parts of the BC and DDAB-BC. To investigate the variation of sorption behavior of BC and DDAB-BC as a function of temperature toward MB removal, the study is carried out in the temperature range from 35 °C (308 K) to 55 °C (328 K), as shown in Figure 7c. The results reveal that for BC, an increase in the sorption capacity (96.84−119.50 mg/g) is observed on increasing the temperature from 308 to 328 K. The same trend has also been observed for DDAB-BC with the only disparity that a higher sorption capacity (136.03−161.92 mg/g) is observed as a function of the change of temperature from 308 to 328 K, thus, the sorption process is endothermic. The endothermic sorption may be credited to the static interactions.[38,39]

2.9. Adsorption Kinetic. Sorption kinetics studies are executed with the intention to establish the mechanism of the MB sorption process onto BC and DDAB-BC. The sorbate molecules are passed through a number of phases: first, transference of sorbate molecules to sorbent (BC and DDAB-BC) surface sites from the solution, for instance shifting of sorbate molecules to the outer surface of the sorbent particles; binding with the exterior sorption sites of the sorbent; and attachment with the sorption sites present in the interior surface parts of the porous region through diffusion.[2,40] Generally, researchers apply a number of kinetics models to determine the sorption mechanism, and the most common kinetics models are pseudo-first-order and pseudo-second-order models.[41−46] The mathematical forms of these models are given below in eqs 1 and 2, and graphical forms are illustrated in Figure 8.

$$\log(q_e - q_t) = \log q_e - \frac{k_1 t}{2.303} \quad (1)$$

$$\frac{t}{q_t} = \frac{1}{k_2 q_e^2} + \frac{t}{q_e} \quad (2)$$

where k_1 (min^{-1}) and k_2 (g/mg.min) are the pseudo-first and pseudo-second-order rate constants, respectively. The experimental results reveal that the pseudo-first-order model, as shown in Figure 8a and Table 1 (R^2 = 0.722 for BC and R^2 = 0.666 for DDAB-BC), is failed to fit well as compared to the pseudo-second-order model, as presented in Figure 8b and Table 1 (R^2 = 0.998 for BC and R^2 = 0.999 for DDAB-BC). Further, the experimental q_e values are closer to the theoretical q_e values calculated from the pseudo-second order model, which also confirms the suitability of the pseudo-second-order model for MB sorption onto BC and DDAB-BC.

Table 1. Kinetic Parameters for Sorption of MB onto BC and DDAB-BC

parameters	BC	DDAB-BC
experimental q_e (mg/g)	122.9	162.4
Pseudo-First-Order		
theoretical q_e (mg/g)	44.65	73.37
$k_1 \times 10^{-3}$ (min^{-1})	10.48	7.139
R^2	0.722	0.666
Pseudo-Second-Order		
theoretical q_e (mg/g)	125.0	163.9
$k_2 \times 10^{-3}$ (g/mg min)	1.185	1.128
R^2	0.998	0.999
Intraparticle Diffusion Model		
region I		
k_{ip} (mg/(g $min^{1/2}$))	8.636	11.10
C_i	87.43	119.2
R^2	0.983	0.981
region II		
k_{ip} (mg/(g $min^{1/2}$))	0.638	0.515
C_i	119.0	159.6
R^2	0.826	0.977

The prediction that the pseudo-second-order kinetics model explains more accurately the sorption of MB is further verified by the literature. Literature confirms that sorption of most of the dyes follows the pseudo-second-order kinetic model.[42,47−49] The pseudo-second-order kinetic model predicts that chemical sorption is the limiting step of MB sorption and thus controls the sorption process.

https://dx.doi.org/10.1021/acsomega.0c01613
ACS Omega 2020, 5, 16711−16721

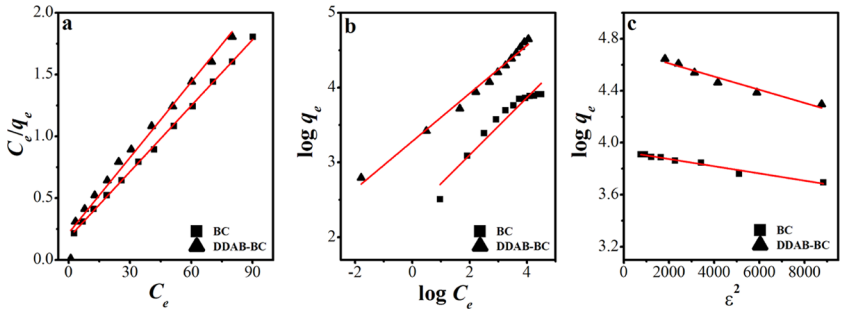

Figure 9. Langmuir model (a), Freundlich model (b), and Dubinin−Raduskevich model (c) for MB sorption onto BC and DDAB-BC.

Weber and Morris in 1963 investigated the direct relation between sorbate sorption and $t^{1/2}$ as an alternative of contact time "t" and is mathematically represented by eq 3

$$q_t = k_{ip}t^{1/2} + C_i \quad (3)$$

where k_{ip} (mg/g.min$^{1/2}$) and C_i represent the intraparticle diffusion rate constant and boundary layer thickness, respectively. When a graph is plotted between q_t and $t^{1/2}$, if it is linear and passes through the origin, then the uptake of sorbate is driven solely by intraparticle diffusion. In the study of sorption behavior of MB, two tendencies reflect that MB uptake is carried out by a combination of other mechanisms alongside intraparticle diffusion (Figure 8c). The first step illustrates that the fast MB uptake occurs at the exterior of the BC and DDAB-BC surface, and the shifting of MB molecules from the solution to the surface sorption sites of the sorbents is accomplished. The second step is the slowest step where the curve moves nearly parallel to the horizontal axis. This second step mainly controls the overall sorption of MB and establishment of equilibrium.[50,51] Further, the greater values of C_i are related to the larger role of the boundary layer effect for the rate-determining step.

2.10. Adsorption Equilibrium. The study of the MB-loaded BC and MB-loaded DDAB-BC equilibrium system affords the interactions between BC and DDAB-BC particles and MB molecules, which provide the basis to design the sorption system.[52,53] Investigations of sorption at constant temperature are utilized to optimize the sorption system and to select the scale. A variety of isothermal models such as Langmuir,[54] Freundlich,[49,55] and Dubinin−Raduskevich (D−R) have been applied for the sorption of MB onto BC and DDAB-BC.[1,56] The mathematical expressions of the Langmuir, Freundlich, and Dubinin−Raduskevich models are represented by eqs 4−7.

$$\frac{C_e}{q_e} = \frac{C_e}{q_m} + \frac{1}{K_L q_m} \quad (4)$$

$$\ln q_e = \ln K_F + \frac{\ln C_e}{n} \quad (5)$$

$$\ln q_e = \ln q_m - K\varepsilon^2 \quad (6)$$

$$E = \frac{1}{\sqrt{2K}} \quad (7)$$

where q_m (mg/g) is the maximum sorption capacity in monolayer sorption. K_L, K_F, and n represent the Langmuir constant, Freundlich constant, and feasibility of the sorption process, respectively. ε is the Polanyi potential, and K is the activity coefficient used to find out the sorption energy E (kJ/mol). The plots of all isotherms are shown in Figure 9, and the values of parameters calculated from all isotherms are shown in Table 2. The R^2 values calculated form the Langmuir, Freundlich, and Dubinin−Raduskevich models are 0.996, 0.939, and 0.803 for BC and 0.997, 0.954, and 0.833 for DDAB-BC, respectively.

Table 2. Adsorption Isotherm Parameters for Sorption of MB onto BC and DDAB-BC

parameters	BC	DDAB-BC
Langmuir		
q_m (mg/g)	123.5	166.7
K_L (L/mg)	0.336	0.899
R_L	0.029	0.100
R^2	0.996	0.997
Freundlich		
K_F (mg/g)(mg/L)$^{1/n}$	36.10	63.28
$1/n$	0.348	0.372
R^2	0.939	0.954
Dubinin−Radushkevich		
q_m (mg/g)	89.26	113.6
$K \times 10^{-6}$ (mol^2/kJ^2)	−0.100	−0.040
E (kJ/mol)	−2.236	−3.535
R^2	0.803	0.833

The comparison of R^2 values shows that the Langmuir model is best fitted and effectively describes the sorption of MB onto BC and DDAB-BC. Furthermore, the suitability of the Langmuir model is also established by the nearness of the theoretical q_m (123.5 mg/g for BC and 166.7 mg/g for DDAB-BC) and experimental q_e (122.9 mg/g for BC and 162.4 mg/g for DDAB-BC). The similar studies and behavior of dye sorption onto different sorbents have been reported by many researchers.[42,49,57,58] Additionally, the values in the range of 1−10 for n (Freundlich constant) also predict favorable MB sorption onto BC and DDAB-BC. The Langmuir model also suggests that MB uptake from the aqueous environment follows the monolayer sorption mechanism, and it is decided using the factor R_L, which is a dimensionless constant.[2] The values of R_L as calculated from the equation ($R_L = 1/1 + K_L C_o$) are between 0 and 1 (R_L = 0.029 for BC and R_L = 0.100 for DDAB-BC), which show that MB uptake onto BC and DDAB-BC is favorable (Table 2).

The D−R model is rooted on the basis that although there are no homogeneous sorbent surface sites but it gives insight into the sorption energy as well as biomass porosity. The values of D−R model constants are presented in Table 2. The values of K are -10×10^{-8} and -4×10^{-8} mol^2/kJ^2 for BC

https://dx.doi.org/10.1021/acsomega.0c01613
ACS Omega 2020, 5, 16711−16721

and DDAB-BC and values of E are −2.236 and −3.535 kJ/mol for BC and DDAB-BC, respectively. The values of E show that the sorption of MB onto BC and DDAB-BC is also showing some contribution of physisorption. Similar behavior has been reported by many authors in their studies.[59,60]

The sorption capacity of DDAB-BC has been compared with that of other adsorbents available in the literature (Table 3), which shows that DDAB-BC evidently reveals excellent sorption performance for MB than other earlier reported adsorbents.

Table 3. Comparison of the Adsorption Capacities of Different Adsorbents for MB Previously Reported with That of DDAB-BC

adsorbent	adsorption capacity (mg/g)	pH	reference
Kaolin	99.90	9.0	72
heteroatom-codoped porous carbon	100.2		73
cross-linked chitosan/bentonite composite	142.9	11.0	74
α-Fe_2O_3@yeast composite	112.7	6.0	75
H_2SO_4 cross-linked magnetic chitosan nanocomposite beads	20.41	6.0	76
Fe_3O_4 activated montmorillonite nanocomposite	106.4	7.4	77
C, N-doped MnO	154.0	9.0	78
Fe_3O_4-CTMAC/SEIA-Mt	246.0		79
DDAB-BC	163.0	7.0	this study

2.11. Adsorption Thermodynamics. A very important factor affecting the sorption of MB on the surface of BC and DDAB-BC is the temperature. The influence of temperature on the sorption behavior of MB onto BC and DDAB-BC is explained by determining the thermodynamic parameters such as standard enthalpy change (ΔH°), standard free energy change (ΔG°), and standard entropy change (ΔS°), using the following mathematical eqs 8 and 9.

$$\Delta G^\circ = -RT \ln K_a \tag{8}$$

$$\ln K_a = \frac{\Delta S^\circ}{R} - \frac{\Delta H^\circ}{RT} \tag{9}$$

where R is the gas constant, T is the temperature in kelvin, and the values of K_a are estimated with respect to temperature by plotting Ln q_e/C_e vs q_e and extra plotting q_e to zero.[61]

The values of ΔS° and ΔH° are calculated from the intercept and slope of the straight-line plot between ln K_a and 1/T, respectively (Figure S4). The values of ΔG° were calculated using eq 8. The values of thermodynamic constants are given in Table 4. The values of ΔG° vary from −2.146 to −3.928 kJ/mol and −5.125 to −11.02 kJ/mol for BC and DDAB-BC, respectively. Thus, values of ΔG° reveal that sorption of MB onto BC and DDAB-BC is spontaneous and feasible at all temperatures. Furthermore, positive values of the ΔS° and ΔH° also show increase in randomness and endothermic nature of MB sorption onto BC and DDAB-BC, which suggests that the sorption process is thermodynamically stable. Moreover, the values of ΔG° slightly decrease at higher temperature, reflecting that the sorption process of MB onto BC and DDAB-BC is more promising at higher temperature.

2.12. FTIR before and after Sorption of MB onto BC and DDAB-BC. Figure 10 shows the FTIR spectra of BC and DDAB-BC before (a,c) and after (b,d) MB sorption. The bands at 1041 and 915 cm^{-1} represent the bending vibrations of Si−O and Al−O, respectively in BC.[62−64] The band at 3627.5 cm^{-1} is attributed to the stretching vibration of the OH group in the BC. The bands at 1467 and 1486 cm^{-1} are assigned to ammonium ions in the DDAB-BC showing the exchange of Na^+ ions by NH_4^+ ions. The bands at 2922.53 and 2852.28 cm^{-1} represent the symmetric and antisymmetric stretching vibrations of CH_2. The band at 1640.38 cm^{-1} represents the water present in the interlayers of the BC. Majority of the bands of the BC and DDAB-BC are analogous to each other, indicating that the original crystal of the DDAB-BC remains the same.[65] The results show that the introduction of DDAB into BC has a stronger interaction with the siloxane surface than the water molecules and hydrated cations in unmodified BC. It was observed that the intensity of the band decreased with the introduction of DDAB. The observed shift of band from HOH bending to CH_2 bending proves that the intercalated surfactant can replace the hydrated cation and shows the hydrophobic properties of the resulting organo-clay.[66−68] Due to the observed changes in the infrared spectrum, it is believed that the interlayer space of BC has been successfully embedded with DDAB.

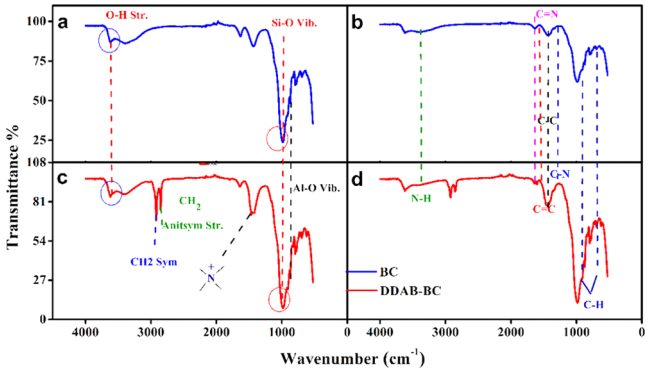

Figure 10. FTIR spectra of (a) BC, (b) MB-loaded BC, (c) DDAB-BC, and (d) MB-loaded DDAB-BC.

Table 4. Thermodynamic Parameters for MB Sorption onto BC and DDAB-BC

	BC			DDAB-BC		
temperature (K)	ΔG° (kJ/mol)	ΔH° (kJ/mol)	ΔS° (J/K mol)	ΔG° (kJ/mol)	ΔH° (kJ/mol)	ΔS° (J/K mol)
308	−2.146			−5.125		
313	−2.592			−6.905		
318	−3.173	25.76	90.67	−8.393	84.84	292.7
323	−3.550			−9.712		
328	−3.928			−11.02		

https://dx.doi.org/10.1021/acsomega.0c01613
ACS Omega 2020, 5, 16711−16721

To confirm MB sorption onto BC and DDAB-BC sorbents, the FTIR analysis is also performed for MB-loaded BC and DDAB-BC samples. Figure 10b,d illustrates the FTIR spectra of MB-loaded BC and DDAB-BC, respectively. The peaks at 1600 and 1450 cm^{-1} represent C═C present in MB, and the peaks at 1690 and 1640 cm^{-1} represent the C═N stretching of MB, which confirms the successful sorption of MB onto BC and DDAB-BC.[69] Further, the peaks at 1300 and 1000 cm^{-1} represent C-O, and peaks at 3500−3300 cm^{-1} represent N−H present in MB.[69] The FTIR spectrum of DDAB-BC shows that as MB interacts with the organoclay, the strength of the two bands (Si−O stretching and CH stretching) increases, indicating an increased organic carbon content between the layers and stronger stretching of siloxane surfaces as well.

3. CONCLUSIONS

In this study, a local BC was modified with a cationic surfactant DDAB to improve its sorption capability to remove MB from the aqueous environment. The results thus obtained have revealed that DDAB-BC has sufficient potential due to acquired properties to be employed as a sorbent for the removal of organic pollutants from water environments. The maximum sorption of MB onto BC and DDAB-BC was found at pH 7, sorbent dose 0.6 g/L, and particle size 74 μm. The sorption equilibrium between MB and DDAB-BC was established in 30 min. Under optimized conditions, the sorption potentials of BC and DDAB-BC for the removal of MB from aqueous environments were 123.5 and 166.7 mg/g, respectively. The isothermal studies showed that MB uptake for BC and DDAB-BC followed the Langmuir isotherm model (R^2 = 0.996 and 0.997) and pseudo-second-order kinetic model (R^2 = 0.998 and 0.999), which fitted well to explain the sorption behavior of MB onto BC and DDAB-BC. Further, for thermodynamics, investigations showed that the sorption process of MB onto BC and DDAB-BC was spontaneous, endothermic in nature, and more favorable at higher elevated temperature. From the results obtained, it may be concluded that the modification of BC with DDAB has successfully improved the sorption properties of the clay. Further, more modification of clays with surfactants could provide new insights into the development of eco-efficient and effective sorbents for the removal of stringent organic pollutants. Hence, bulk availability of BC at a local level boosts its applicability as a cost-effective and highly economical source of cleaner production.

4. EXPERIMENTAL SECTION

4.1. Sorbent Preparation. Eight different clay samples were obtained from the areas of northern Punjab and Bhember AJK, Pakistan. The names of clays are green clay (GC), natural pink clay (NPC), sky blue clay (SBC), black clay (BkC), gray clay (GyC), brown clay (BC), red clay (RC), and light yellow clay (LtYC). All of the clays were ground into a fine powder using pestle and mortar. Further, clays were dried by keeping in an oven for a 24 h time period (at 105 °C) to evaporate the moisture and were then preserved in airtight containers. After the preliminary study, BC was found to be more efficient for the removal of MB, so it was selected for further study. BC was further refined into an amorphous powder to collect different particle sizes utilizing grading sieves. The sorbent was dried by keeping in an oven for a 24 h time period to evaporate the moisture and was then kept in airtight containers. Chemical composition of BC as examined is given in Table S2.

DDAB-BC was prepared by intercalation of the clay with cationic surfactant DDAB according to the method given in the literature.[70] Briefly, 10 g of BC was suspended in 1.0 L of deionized water. The mixture was continuously agitated for a 24 h time period at ambient conditions utilizing a magnetic stirrer. The solution of DDAB tantamount to the cation-exchange capacity (CEC) of the clay was prepared, and the required quantity of DDAB was added to the BC suspension to carry out the positive ion exchange reaction. The suspension of DDAB-BC was further stirred for an interval of 12 h, and then water was removed from DDAB-BC using vacuum filtration. Residual chloride and other ions were removed from DDAB-BC by adding fresh deionized water and stirring for a 6 h time period. The process of rinsing was repeated until the absence of chloride, which was confirmed with a silver nitrate ($AgNO_3$) solution. The acquired DDAB-BC was dried under vacuum, at 60 °C for 24 h, and ground by a pestle and mortar into a fine powder.

4.2. Sorbent Characterization. Inert BC and DDAB-BC sorbents were characterized using suitable analytical techniques. Through the BET method, exploiting N_2 sorption isotherms (at 77 K), the pore diameter and specific surface area were estimated by a pore size and surface area analyzer. Exploiting the Barrett−Joyner−Halenda (BJH) route, pore distributions of BC and DDAB-BC were computed. The gases were removed from BC and DDAB-BC using a sonicator degasser prior to accomplishment of surface analyses. The morphological structures of BC and DDAB-BC samples were visually appraised from the data acquired by a JSM 5 × 910 instrument (JEOL, Japan), i.e., SEM micrographs. To determine the type of functional groups existing on BC and DDAB-BC, FTIR analysis was carried out exploiting a FTIR spectrometer (Jasco, USA). XRD spectra for BC and DDAB-BC were obtained using Cu Kα radiation (Cu anode, Kα_1 wavelength 1.540598, Kα_2 wavelength 1.5444426 such that the ratio of Kα_2 to Kα_1 was 0.5) operated at a generator voltage of 40 kV and tube current of 30 mA. The pH_{pzc} was determined by the drift route as reported in the literature.[71] Suitable concentrations (0.1 M) of both NaOH and HCl solutions were added systematically to regulate the pH.

4.3. Sorption Studies. MB was obtained from the market and was utilized in the experimental investigations without any purification treatment. The stock solution of 1000 mg/L of MB ($C_{16}H_{18}ClN_3S$ and M = 319.85 g/mol) was prepared by dissolving accurately measured 1.0 g of MB per 1000 mL of doubly distilled water. This stock solution was used to prepare the standard experimental solutions diluted by distilled water. A UV/vis spectrophotometer (PG Instrument T60, U.K.) was used to measure the absorbance of the MB solutions at 670 nm wavelength.

Sorption studies were conducted using the batch method to explore the influence of applied factors such as pH, sorbent dosage, temperature, initial dye concentration, and contact time on the sorption of MB onto BC and DDAB-BC sorbents. The experimental criteria such as pH (2−11), sorbent particle size (37−400 μm), MB concentration (10−110 mg/L), BC and DDAB-BC dose (0.4−2.4 g/L), temperature (35−55 °C), and contact time (2−45 min) were evaluated exploiting the one-factor one-time approach. For each single batch, 100 mL portion of the MB sorbate solution was shaken in a 250 mL titration flask with a weighed amount of BC and DDAB-BC

https://dx.doi.org/10.1021/acsomega.0c01613
ACS Omega 2020, 5, 16711−16721

sorbents for a definite time period at predefined conditions. The details of each run were mentioned in the relative portion of result and discussion. The optimum set of experimental conditions used in all of the experiments, unless otherwise specified, are as follows: sorbent dose (0.6 g/L), sorbate concentration (100 mg/L), contact time (30 min), pH 7, temperature (55 °C), and stirring speed (200 ppm). An orbital shaker has been utilized to equilibrate the MB-BC and MB-DDAB-BC heterogeneous systems. After equilibrating, the heterogeneous systems (MB-BC and MB-DDAB-BC) were subjected to centrifugation and filtration. The residual MB concentration was determined using a spectrophotometer by analyzing the filtrate. The residual MB concentration was used to determine the sorption capacity q_e (mg/g) exploiting eq 10

$$q_e = \frac{(C_0 - C_e)V}{w} \tag{10}$$

where C_e (mg/L) is the MB concentration at equilibrium, C_o (mg/L) is the initial MB concentration, w (g) is the sorbent mass, and V (L) is the MB solution volume. All of the experiments were performed in triplicate. The results were reported as mean ± SD.

The quantity of MB uptake q_t (mg/g) at time "t" was acquired exploiting eq 11

$$q_t = \frac{(C_0 - C_t)V}{w} \tag{11}$$

where q_t (mg/g) and C_t (mg/L) represent the amount of MB sorbed and MB concentration at any instant time "t", respectively.

■ ASSOCIATED CONTENT

Supporting Information

The Supporting Information is available free of charge at https://pubs.acs.org/doi/10.1021/acsomega.0c01613.

Molecular structure of MB; the BET isotherm plot of BC; BET surface parameters of BC and DDAB-BC; composition of BC; the point of zero charge (pHPZC) of BC and DDAB-BC sorbents; and plots of Ln K_a vs 1/T for MB sorption onto BC and DDAB-BC (PDF)

■ AUTHOR INFORMATION

Corresponding Authors

Muhammad Faizan Nazar − *Department of Chemistry, University of Gujrat, Gujrat 50700, Pakistan*; Email: faizan.nazar@uog.edu.pk

Muhammad Nadeem Zafar − *Department of Chemistry, University of Gujrat, Gujrat 50700, Pakistan*; orcid.org/0000-0002-2109-7601; Email: znadeempk@gmail.com, nadeem.zafar@uog.edu.pk

Authors

Muhammad Munir − *Department of Chemistry, University of Gujrat, Gujrat 50700, Pakistan*

Muhammad Zubair − *Department of Chemistry, University of Gujrat, Gujrat 50700, Pakistan*

Muhammad Ashfaq − *Department of Chemistry, University of Gujrat, Gujrat 50700, Pakistan*

Ahmad Hosseini-Bandegharaei − *Department of Environmental Health Engineering, Faculty of Health, Sabzevar University of Medical Sciences, Sabzevar, Iran; Department of Engineering, Kashmar Branch, Islamic Azad University, Kashmar, Iran*

Salah Ud-Din Khan − *Sustainable Energy Technologies Center, King Saud University, Riyadh 11421, Saudi Arabia*

Ashfaq Ahmad − *Department of Chemistry, King Saud University, Riyadh 11451, Saudi Arabia*

Complete contact information is available at: https://pubs.acs.org/10.1021/acsomega.0c01613

Notes

The authors declare no competing financial interest.

■ ACKNOWLEDGMENTS

The authors express their gratitude to the Department of Chemistry, University of Gujrat, Pakistan, for the provision of lab facility. The authors acknowledge financial support from the Higher Education Commission of Pakistan through NRPU projects (20-4557/NRPU/R&D/HEC/14/481 and 6515/Punjab/NRPU/R&D/HEC/2016). The authors also appreciate funding from the Researchers Supporting Project (RSP-2020/58) from the King Saud University, Riyadh, Saudi Arabia.

■ REFERENCES

(1) Rehman, M. S. U.; Munir, M.; Ashfaq, M.; Rashid, N.; Nazar, M. F.; Danish, M.; Han, J.-I. Adsorption of Brilliant Green dye from aqueous solution onto red clay. *Chem. Eng. J.* **2013**, *228*, 54−62.

(2) Safa, Y.; Bhatti, H. N. Kinetic and thermodynamic modeling for the removal of Direct Red-31 and Direct Orange-26 dyes from aqueous solutions by rice husk. *Desalination* **2011**, *272*, 313−322.

(3) Auta, M.; Hameed, B. Preparation of waste tea activated carbon using potassium acetate as an activating agent for adsorption of Acid Blue 25 dye. *Chem. Eng. J.* **2011**, *171*, 502−509.

(4) Qian, F.; Sun, X.; Liu, Y. Removal characteristics of organics in bio-treated textile wastewater reclamation by a stepwise coagulation and intermediate GAC/O3 oxidation process. *Chem. Eng. J.* **2013**, *214*, 112−118.

(5) Javaid, M.; Saleemi, A. R.; Naveed, S.; Zafar, M.; Ramzan, N. Anaerobic treatment of desizing effluent in a mesophilic anaerobic packed bed reactor. *J. Pak. Inst. Chem. Eng.* **2011**, *39*, 61−67.

(6) Aziz, F.; Rehman, M. S.; Batool, A.; Muhammad, A.; Mahmood, T. Pretreatment of municipal, industrial and composite wastewater by ozonation. *Environ. Process Eng.* **2012**, *1*, 1−8.

(7) Kurt, E.; Koseoglu-Imer, D. Y.; Dizge, N.; Chellam, S.; Koyuncu, I. Pilot-scale evaluation of nanofiltration and reverse osmosis for process reuse of segregated textile dyewash wastewater. *Desalination* **2012**, *302*, 24−32.

(8) Yasar, A.; Khalil, S.; Tabinda, A. B.; Malik, A. Comparison of cost and treatment efficiency of solar assisted advance oxidation processes for textile dye bath effluent. *Korean J. Chem. Eng.* **2013**, *30*, 131−138.

(9) Zafar, M. N.; Aslam, I.; Nadeem, R.; Munir, S.; Rana, U. A.; Khan, S. U. D. Characterization of chemically modified biosorbents from rice bran for biosorption of Ni(II). *J. Taiwan Inst. Chem. Eng.* **2015**, *46*, 82−88.

(10) Liu, Y.; Wang, S.; Lu, Y.; Zhao, Y.; Zhang, Y.; Xu, G.; Zhang, J.; Fang, Z.; Xu, W.; Chen, X. Loading Control of Metal−Organic Frameworks in Fe3O4@MOFs Series Composite Adsorbents for Optimizing Dye Adsorption. *Ind. Eng. Chem. Res.* **2019**, *58*, 22244−22249.

(11) Rehman, M. S. U.; Kim, I.; Han, J.-I. Adsorption of methylene blue dye from aqueous solution by sugar extracted spent rice biomass. *Carbohydr. Polym.* **2012**, *90*, 1314−1322.

(12) Rehman, M. S. U.; Han, J.-I. Biosorption of methylene blue from aqueous solutions by Typha angustata phytomass. *Int. J. Environ. Sci. Technol.* **2013**, *10*, 865−870.

(13) Bulgariu, L.; Escudero, L. B.; Bello, O. S.; Iqbal, M.; Nisar, J.; Adegoke, K. A.; Alakhras, F.; Kornaros, M.; Anastopoulos, I. The utilization of leaf-based adsorbents for dyes removal: A review. *J. Mol. Liq.* **2019**, *276*, 728−747.
(14) Auta, M.; Hameed, B. Modified mesoporous clay adsorbent for adsorption isotherm and kinetics of methylene blue. *Chem. Eng. J.* **2012**, *198*, 219−227.
(15) Auta, M.; Hameed, B. Acid modified local clay beads as effective low-cost adsorbent for dynamic adsorption of methylene blue. *J. Ind. Eng. Chem.* **2013**, *19*, 1153−1161.
(16) Kismir, Y.; Aroguz, A. Z. Adsorption characteristics of the hazardous dye Brilliant Green on Saklıkent mud. *Chem. Eng. J.* **2011**, *172*, 199−206.
(17) Nassar, M. M.; El-Geundi, M. S.; Al-Wahbi, A. A. Equilibrium modeling and thermodynamic parameters for adsorption of cationic dyes onto Yemen natural clay. *Desalin. Water Treat.* **2012**, *44*, 340−349.
(18) Bai, T.; Zhao, K.; Gao, Q.; Qi, M.; Zhang, Y.; Lu, Z.; Zhao, H.; Gao, H.; Wei, J. Kaolin/CaAlg Hydrogel Thin Membrane with Controlled Thickness, High Mechanical Strength, and Good Repetitive Adsorption Performance for Dyes. *Ind. Eng. Chem. Res.* **2020**, *59*, 4958−4967.
(19) Yaqoob, S.; Ullah, F.; Mehmood, S.; Mahmood, T.; Ullah, M.; Khattak, A.; Zeb, M. A. Effect of waste water treated with TiO2 nanoparticles on early seedling growth of Zea mays L. *J. Water Reuse Desalin.* **2018**, *8*, 424−431.
(20) Boyd, S. A.; Mortland, M. M.; Chiou, C. T. Sorption characteristics of organic compounds on hexadecyltrimethylammonium-smectite. *Soil Sci. Soc. Am. J.* **1988**, *52*, 652−657.
(21) Ozola, R.; Krauklis, A.; Burlakovs, J.; Klavins, M.; Vincevica-Gaile, Z.; Hogland, W. Surfactant-Modified Clay Sorbents for the Removal of p-nitrophenol. *Clays Clay Miner.* **2019**, *67*, 132−142.
(22) Dutta, A.; Singh, N. Surfactant-modified bentonite clays: preparation, characterization, and atrazine removal. *Environ. Sci. Pollut. Res.* **2015**, *22*, 3876−3885.
(23) Sun, K.; Shi, Y.; Chen, H.; Wang, X.; Li, Z. Extending surfactant-modified 2:1 clay minerals for the uptake and removal of diclofenac from water. *J. Hazard. Mater.* **2017**, *323*, 567−574.
(24) Zawrah, M. F.; Khattab, R. M.; Saad, E. M.; Gado, R. A. Effect of surfactant types and their concentration on the structural characteristics of nanoclay. *Spectrochim. Acta, Part A* **2014**, *122*, 616−623.
(25) Saitoh, T.; Shibayama, T. Removal and degradation of β-lactam antibiotics in water using didodecyldimethylammonium bromide-modified montmorillonite organoclay. *J. Hazard. Mater.* **2016**, *317*, 677−685.
(26) Ahmadishoar, J.; Bahrami, H. S.; Movassagh, B.; Amirshahi, H. S.; Arami, M. Removal of Disperse Blue 56 and Disperse Red 135 dyes from aqueous dispersions by modified montmorillonite nanoclay. *Chem. Ind. Chem. Eng. Q.* **2017**, *23*, 21−29.
(27) Balarak, D.; Jaafari, J.; Hassani, G.; Mahdavi, Y.; Tyagi, I.; Agarwal, S.; Gupta, V. K. The use of low-cost adsorbent (Canola residues) for the adsorption of methylene blue from aqueous solution: Isotherm, kinetic and thermodynamic studies. *Colloids Interface Sci. Commun.* **2015**, *7*, 16−19.
(28) Abd El-Ghaffar, M. A.; Youssef, A.; El-Hakim, A. A. Polyaniline nanocomposites via in situ emulsion polymerization based on montmorillonite: Preparation and characterization. *Arabian J. Chem.* **2015**, *8*, 771−779.
(29) Bhattacharyya, K. G.; Sharma, A. Kinetics and thermodynamics of methylene blue adsorption on neem (Azadirachta indica) leaf powder. *Dyes Pigm.* **2005**, *65*, 51−59.
(30) Beltrán-Suito, R.; Pinedo-Flores, A.; Bravo-Hualpa, F.; Ramos-Muñoz, J.; Sun-Kou, M. d. R. Adsorption of N, N-dimethylamine from aqueous solutions by a metal organic framework, MOF−235. *J. Disp. Sci. Technol.* **2018**, 1−8.
(31) Reddy, D. D.; Ghosh, R. K.; Bindu, J. P.; Mahadevaswamy, M.; Murthy, T. Removal of methylene blue from aqueous system using tobacco stems biomass: Kinetics, mechanism and single-stage adsorber design. *Environ. Prog. Sustainable Energy* **2017**, *36*, 1005−1012.
(32) Reske, R.; Mistry, H.; Behafarid, F.; Roldan Cuenya, B.; Strasser, P. Particle size effects in the catalytic electroreduction of CO2 on Cu nanoparticles. *J. Am. Chem. Soc.* **2014**, *136*, 6978−6986.
(33) Gupta, V. K.; Jain, R.; Mittal, A.; Saleh, T. A.; Nayak, A.; Agarwal, S.; Sikarwar, S. Photo-catalytic degradation of toxic dye amaranth on TiO 2/UV in aqueous suspensions. *Mater. Sci. Eng.: C* **2012**, *32*, 12−17.
(34) Ahmad, R.; Kumar, R. Adsorption of amaranth dye onto alumina reinforced polystyrene. *Clean Soil, Air, Water.* **2011**, *39*, 74−82.
(35) Mane, V. S.; Babu, P. V. Kinetic and equilibrium studies on the removal of Congo red from aqueous solution using Eucalyptus wood (Eucalyptus globulus) saw dust. *J. Taiwan Inst. Chem. Eng.* **2013**, *44*, 81−88.
(36) El-Bindary, A. A.; El-Sonbati, A. Z.; Al-Sarawy, A. A.; Mohamed, K. S.; Farid, M. A. Adsorption and thermodynamic studies of hazardous azocoumarin dye from an aqueous solution onto low cost rice straw based carbons. *J. Mol. Liq.* **2014**, *199*, 71−78.
(37) El-Bindary, A. A.; Hussien, M. A.; Diab, M. A.; Eessa, A. M. Adsorption of Acid Yellow 99 by polyacrylonitrile/activated carbon composite: kinetics, thermodynamics and isotherm studies. *J. Mol. Liq.* **2014**, *197*, 236−242.
(38) Yao, Y.; Xu, F.; Chen, M.; Xu, Z.; Zhu, Z. Adsorption behavior of methylene blue on carbon nanotubes. *Bioresour. Technol.* **2010**, *101*, 3040−3046.
(39) Ho, Y.-S.; McKay, G. Sorption of dye from aqueous solution by peat. *Chem. Eng. J.* **1998**, *70*, 115−124.
(40) Mane, V. S.; Babu, P. V. Studies on the adsorption of Brilliant Green dye from aqueous solution onto low-cost NaOH treated saw dust. *Desalination* **2011**, *273*, 321−329.
(41) Ho, Y.; Ng, J.; McKay, G. Kinetics of pollutant sorption by biosorbents: review. *Sep. Purif. Methods* **2000**, *29*, 189−232.
(42) Zafar, M. N.; Amjad, M.; Tabassum, M.; Ahmad, I.; Zubair, M. SrFe2O4 nanoferrites and SrFe2O4/ground eggshell nanocomposites: Fast and efficient adsorbents for dyes removal. *J. Clean. Prod.* **2018**, *199*, 983−994.
(43) Lagergren, S. About the theory of so-called adsorption of soluble substances. *Kungliga Svenska Vetenskapsakad Handlngar* **1898**, *24*, 1−39.
(44) Ho, Y. S.; McKay, G. Pseudo-second order model for sorption processes. *Process Biochem.* **1999**, *34*, 451−465.
(45) Zafar, M. N.; Abbas, I.; Nadeem, R.; Sheikh, M. A.; Ghauri, M. A. Removal of Nickel onto Alkali Treated Rice Bran. *Water, Air, Soil Pollut.* **2009**, *197*, 361−370.
(46) Kumari, S.; Khan, A. A.; Chowdhury, A.; Bhakta, A. K.; Mekhalif, Z.; Hussain, S. Efficient and highly selective adsorption of cationic dyes and removal of ciprofloxacin antibiotic by surface modified nickel sulfide nanomaterials: Kinetics, isotherm and adsorption mechanism. *Colloids Surf., A* **2020**, *586*, No. 124264.
(47) Abdellaoui, K.; Pavlovic, I.; Bouhent, M.; Benhamou, A.; Barriga, C. A comparative study of the amaranth azo dye adsorption/desorption from aqueous solutions by layered double hydroxides. *Appl. Clay Sci.* **2017**, *143*, 142−150.
(48) Nasuha, N.; Hameed, B. Adsorption of methylene blue from aqueous solution onto NaOH-modified rejected tea. *Chem. Eng. J.* **2011**, *166*, 783−786.
(49) Zafar, M. N.; Dar, Q.; Nawaz, F.; Zafar, M. N.; Iqbal, M.; Nazar, M. F. Effective adsorptive removal of azo dyes over spherical ZnO nanoparticles. *J. Mater. Res. Technol.* **2019**, *8*, 713−725.
(50) Sreenivasulu, B.; Sreedhar, I.; Venugopal, A.; Reddy, B. M.; Raghavan, K. V. Thermo-kinetic investigations of high temperature carbon capture using Coal-Flyash doped sorbent. *Energy Fuels* **2017**, DOI: 10.1021/acs.energyfuels.6b02721.
(51) Pan, M.; Lin, X.; Xie, J.; Huang, X. Kinetic, equilibrium and thermodynamic studies for phosphate adsorption on aluminum hydroxide modified palygorskite nano-composites. *RSC Adv.* **2017**, *7*, 4492−4500.

https://dx.doi.org/10.1021/acsomega.0c01613
ACS Omega 2020, 5, 16711−16721

(52) Kavitha, D.; Namasivayam, C. Experimental and kinetic studies on methylene blue adsorption by coir pith carbon. *Bioresour. Technol.* **2007**, *98*, 14−21.
(53) Ghaedi, M.; Hossainian, H.; Montazerozohori, M.; Shokrollahi, A.; Shojaipour, F.; Soylak, M.; Purkait, M. A novel acorn based adsorbent for the removal of brilliant green. *Desalination* **2011**, *281*, 226−233.
(54) Langmuir, I. The adsorption of gases on plane surfaces of glass, mica and platinum. *J. Am. Chem. Soc.* **1918**, *40*, 1361−1403.
(55) Freundlich, H. Adsorption in solutions. *J. Phys. Chem. A* **1906**, *57*, 384−410.
(56) Gardner, L.; Kruk, M.; Jaroniec, M. Reference data for argon adsorption on graphitized and nongraphitized carbon blacks. *J. Phys. Chem. B* **2001**, *105*, 12516−12523.
(57) Kipling, J. J. *Adsorption from Solutions of Non-Electrolytes*; Academic Press, 2017.
(58) Li, L.; Liu, F.; Jing, X.; Ling, P.; Li, A. Displacement mechanism of binary competitive adsorption for aqueous divalent metal ions onto a novel IDA-chelating resin: isotherm and kinetic modeling. *Water Res.* **2011**, *45*, 1177−1188.
(59) Abia, A.; Horsfall, M.; Didi, O. The use of chemically modified and unmodified cassava waste for the removal of Cd, Cu and Zn ions from aqueous solution. *Bioresour. Technol.* **2003**, *90*, 345−348.
(60) Elinge, C.; Itodo, A.; Peni, I.; Birnin-Yauri, U.; Mbongo, A. Assessment of heavy metals concentrations in bore-hole waters in Aliero community of Kebbi State. *Adv. Appl. Sci. Res.* **2011**, *2*, 279−282.
(61) Zubair, M.; Jarrah, N.; Manzar, M. S.; Al-Harthi, M.; Daud, M.; Mu'azu, N. D.; Haladu, S. A. Adsorption of eriochrome black T from aqueous phase on MgAl-, CoAl- and NiFe- calcined layered double hydroxides: Kinetic, equilibrium and thermodynamic studies. *J. Mol. Liq.* **2017**, *230*, 344−352.
(62) Zhou, Q.; He, H. P.; Zhu, J. X.; Shen, W.; Frost, R. L.; Yuan, P. Mechanism of p-nitrophenol adsorption from aqueous solution by HDTMA + -pillared montmorillonite—implications for water purification. *J. Hazard. Mater.* **2008**, *154*, 1025−1032.
(63) Zhou, K.; Liu, J.; Zeng, W.; Hu, Y.; Gui, Z. In situ synthesis, morphology, and fundamental properties of polymer/MoS 2 nanocomposites. *Compos. Sci. Technol.* **2015**, *107*, 120−128.
(64) Peng, K.; Fu, L.; Li, X.; Ouyang, J.; Yang, H. Stearic acid modified montmorillonite as emerging microcapsules for thermal energy storage. *Appl. Clay Sci.* **2017**, *138*, 100−106.
(65) Yuan, P.; Annabi-Bergaya, F.; Tao, Q.; Fan, M.; Liu, Z.; Zhu, J.; He, H.; Chen, T. A combined study by XRD, FTIR, TG and HRTEM on the structure of delaminated Fe-intercalated/pillared clay. *J. Colloid Interface Sci.* **2008**, *324*, 142−149.
(66) He, H.; Frost, R. L.; Bostrom, T.; Yuan, P.; Duong, L.; Yang, D.; Xi, Y.; Kloprogge, J. T. Changes in the morphology of organoclays with HDTMA+ surfactant loading. *Appl. Clay Sci.* **2006**, *31*, 262−271.
(67) He, H.; Yang, D.; Yuan, P.; Shen, W.; Frost, R. L. A novel organoclay with antibacterial activity prepared from montmorillonite and Chlorhexidini Acetas. *J. Colloid Interface Sci.* **2006**, *297*, 235−243.
(68) He, H.; Zhou, Q.; Martens, W. N.; Kloprogge, T. J.; Yuan, P.; Xi, Y.; Zhu, J.; Frost, R. L. Microstructure of HDTMA+-modified montmorillonite and its influence on sorption characteristics. *Clays Clay Miner.* **2006**, *54*, 689−696.
(69) Ghodake, G.; Jadhav, U.; Tamboli, D.; Kagalkar, A.; Govindwar, S. Decolorization of textile dyes and degradation of mono-azo dye amaranth by Acinetobacter calcoaceticus NCIM 2890. *Indian J. Microbiol.* **2011**, *51*, 501−508.
(70) He, H.; Ma, Y.; Zhu, J.; Yuan, P.; Qing, Y. Organoclays prepared from montmorillonites with different cation exchange capacity and surfactant configuration. *Appl. Clay Sci.* **2010**, *48*, 67−72.
(71) Çakmak, M.; Taşar, Ş.; Selen, V.; Özer, D.; Özer, A. Removal of astrazon golden yellow 7GL from colored wastewater using chemically modified clay. *J. Central South Univ.* **2017**, *24*, 743−753.
(72) Mouni, L.; Belkhiri, L.; Bollinger, J.-C.; Bouzaza, A.; Assadi, A.; Tirri, A.; Dahmoune, F.; Madani, K.; Remini, H. Removal of Methylene Blue from aqueous solutions by adsorption on Kaolin: Kinetic and equilibrium studies. *Appl. Clay Sci.* **2018**, *153*, 38−45.
(73) Chen, B.; Yang, Z.; Ma, G.; Kong, D.; Xiong, W.; Wang, J.; Zhu, Y.; Xia, Y. Heteroatom-doped porous carbons with enhanced carbon dioxide uptake and excellent methylene blue adsorption capacities. *Microporous Mesoporous Mater.* **2018**, *257*, 1−8.
(74) Bulut, Y.; Karaer, H. Adsorption of Methylene Blue from Aqueous Solution by Crosslinked Chitosan/Bentonite Composite. *J. Dispersion Sci. Technol.* **2015**, *36*, 61−67.
(75) Wang, Y.; Zhang, W.; Qin, M.; Zhao, M.; Zhang, Y. Green one-pot preparation of α-Fe2O3@carboxyl-functionalized yeast composite with high adsorption and catalysis properties for removal of methylene blue. *Surf. Interface Anal.* **2018**, *50*, 311−320.
(76) Rahmi; Ishmaturrahmi; Mustafa, I. Methylene blue removal from water using H2SO4 crosslinked magnetic chitosan nanocomposite beads. *Microchem. J.* **2019**, *144*, 397−402.
(77) Chang, J.; Ma, J.; Ma, Q.; Zhang, D.; Qiao, N.; Hu, M.; Ma, H. Adsorption of methylene blue onto Fe3O4/activated montmorillonite nanocomposite. *Appl. Clay Sci.* **2016**, *119*, 132−140.
(78) Xu, Y.; Ren, B.; Wang, R.; Zhang, L.; Jiao, T.; Liu, Z. Facile Preparation of Rod-like MnO Nanomixtures via Hydrothermal Approach and Highly Efficient Removal of Methylene Blue for Wastewater Treatment. *Nanomaterials* **2019**, *9*, No. 10.
(79) Rahmani, S.; Zeynizadeh, B.; Karami, S. Removal of cationic methylene blue dye using magnetic and anionic-cationic modified montmorillonite: kinetic, isotherm and thermodynamic studies. *Appl. Clay Sci.* **2020**, *184*, No. 105391.

https://dx.doi.org/10.1021/acsomega.0c01613
ACS Omega 2020, 5, 16711−16721